Advances in Manufacturing Technology XXXIV
M. Shafik and K. Case (Eds.)

doi:10.3233/ATDE210035

Creep-Fatigue Behaviours of Sn-Ag-Cu Solder Joints in Microelectronics Applications

Joshua A. Depiver [a,1], Sabuj Mallik [a,2], Yiling Lu [a] , and Emeka H. Amalu [b]
[a] *Department of Mechanical Engineering & Built Environment, College of Engineering & Technology, University of Derby, Markeaton Street, Derby, DE22 3AW UK*
[b] *Department of Mechanical Engineering, School of Science, Engineering & Design, Teesside University, Middlesbrough, Tees Valley, TS1 3BX, UK*

Abstract. Electronic manufacturing is one of the dynamic industries in the world in terms of leading technological advancements. Electronic assembly's heart lies the 'soldering technology' and the 'solder joints' between electronic components and substrate. During the operation of electronic products, solder joints experience harsh environmental conditions in terms of cyclic change of temperature and vibration and exposure to moisture and chemicals. Due to the cyclic application of loads and higher operational temperature, solder joints fail primarily through creep and fatigue failures. This paper presents the creep-fatigue behaviours of solder joints in a ball grid array (BGA) soldered on a printed circuit board (PCB). Using finite element (FE) simulation, the solder joints were subjected to thermal cycling and isothermal ageing. Accelerated thermal cycling (ATC) was carried out using a temperate range from 40℃ to 150℃, and isothermal ageing was done at $-40, 25, 75$ and 150℃ temperatures for 45 days (64,800 mins). The solders studied are lead-based eutectic Sn63Pb37 and lead-free SAC305, SAC387, SAC396 and SAC405. The results were analysed using the failure criterion of equivalent stress, strain rate, deformation rate, and the solders' strain energy density. The SAC405 and SAC396 have the least stress magnitude, strain rate, deformation rate, and strain energy density damage than the lead-based eutectic Sn63Pb37 solder; they have the highest fatigue lives based on the damage mechanisms. This research provides a technique for determining the preventive maintenance time of BGA components in mission-critical systems. Furthermore, it proposes developing a new life prediction model based on a combination of the damage parameters for improved prediction.

Keywords. Creep, Fatigue, Thermal cycling, Isothermal ageing, Stress, Strain

1. Introduction

Solder joints exhibit creep and fatigue behaviour that depends on the thermal environment, solder joint configuration, and solder alloy properties even at room temperature. Ensuring the reliability of solder joints in electronic devices is fundamental for the operational performance of electronics systems used in safety-critical applications such as aerospace, defence, oil, & gas drilling, underhood of automobiles, medical devices, and power grids. Many parameters assess the reliability of solder joints: shear strength, creep resistance, drop shock, thermal fatigue, and vibration resistance. Due to

[1] Corresponding Author. J.depiver@derby.ac.uk / jdepiver@aol.com
[2] Corresponding Author. s.mallik@derby.ac.uk

the implementation of the Restriction of Hazardous Substances (RoHS) directives on July 1, 2006, by the European Union (EU), there have been new progress and developments in lead-free solders as a replacement for the conventional lead-based solders for application in the electronics manufacturing industries [1], [2].

Electronic device loading during field operations can be modelled using thermal cycling and isothermal ageing. Thermal ageing of solder joints produces changes in solder microstructure which triggers creep failure [3]. Temperature cycling creates thermal stress in the solder joints, which culminates in fatigue failure. Solder alloy materials are extensively used in electronic packaging because they have low melting temperature and excellent wetting properties. During electronic devices service life, a mismatch of thermal expansion coefficient (CTE) of different materials bonded together in the assembly causes cycling stresses and strain in their solder joints. The solder joints also deteriorate due to creep response, depending on temperature, ageing, stress, strain, and solder grain size. The response is modelled using a variety of creep relations based on the Garofalo model. Constitutive models employed for solder alloys have been reported by Basaran et al. [4] and Gomez and Basaran [5]. An analysis of the models shows that a solder alloy's creep behaviour depends on age, stress, temperature, and solder grain size. Fatigue is dominant during cycling between the extremes, so creep dominates during the dwelling period and at high temperatures. The effect of ageing on the cyclic stress-strain, the degradation of isothermal failure resulting from ageing and thermal fatigue life has been investigated in this paper for lead-based eutectic Sn63Pb37 and four lead-free solders (SAC305, SAC387, SAC396 and SAC405).

As temperature cycling drives fatigue failure of solder joints in electronic modules, characterisation of the thermal fatigue response of different solder alloy formulations in BGA solder joints functioning in mission-critical systems has become crucial. Four different lead-free and one eutectic lead-based solder alloys in BGA solder joints are characterised against their thermal fatigue lives (TFLs) to predict their mean-time-to-failure for preventive maintenance advice. Five finite elements (FE) models of the assemblies of the BGAs with the different solder alloy compositions are created with SolidWorks. Plastic strain, shear strain, plastic shear strain, and accumulated creep energy density responses of the solder joints are obtained and inputted into established life prediction models – Coffin Manson, Engelmaier, Solomon and Syed – to determine the fatigue lives of the solder alloys considered in this work for low cycle fatigue (LCF).

2. Methodology

2.1 Mesh Convergence and Independent study

Mesh convergence study is carried out using the three steps below:

Step 1: Create a mesh using the fewest, reasonable number of elements and analyse the model.

Step 2: Recreate the mesh with a denser element distribution, re-analyse it, and compare the previous mesh results in step 1.

Step 3: Keep increasing the mesh density and re-analysing the model until the results converge satisfactorily [Fig 1].

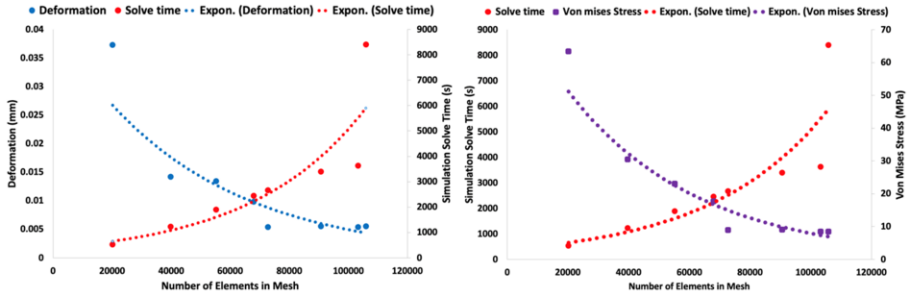

Figure 1: Trend line of convergence vs simulation solve time for Deformation and Von mises Stress of lead-free SAC305 solder alloy showing the asymptotic line

2.2 Finite element modelling (FEM)

The FEM utilising finite element analysis (FEA) has been widely and successfully employed to conduct research investigations on thermo-mechanical reliability of electronic components mounted on PCB. This section presents the modelling procedure implemented in carrying out the study.

2.2.1 Materials properties and model equations

The BGA assembly materials and their mechanical properties are presented in author publications [6]–[8]. In addition, the material properties are obtained from several high-impact peer-reviewed literatures. The assembly's critical component material includes solder alloys, Copper (Cu) pad, epoxy-resin board, mask, and silicon (Si) die. All the materials were modelled as linear elastic and isotropic substances except the PCB, and the solder alloys, simulated using the orthographic material properties and Garofalo creep relations. The thermo-mechanical behaviour of the silicon (Si) die, epoxy-resin board, Copper (Cu) pad and mask were modelled as isotropic, linear elastic and temperature independent. To limit the simulation time for accurate results and fewer errors, only the solder joint alloys were modelled as non-linear behaviour.

Furthermore, the available published constitutive properties of lead-free solder alloys are limited, and validation of some existing models is still ongoing. For this study, lead-based solder alloy's creep behaviour is assumed to obey the Garofalo-Arrhenius creep constitutive law. The materials properties and constants could be accessed in the authors' publications [7], [8].

The Garofalo Hyperbolic Sine Law [9] is stated thus:

$$\dot{\varepsilon} = A[\sinh(\alpha\sigma)]^n e^{\left(-\frac{Q}{RT}\right)} \quad (1)$$

where $\dot{\varepsilon}$ is creeping strain rate, A is a material constant, α is a multiplier of hyperbolic-sine law, which is obtained from curve fitting to experimental data by using linear and non-linear least square regression, σ is the applied shear stress, n is the stress exponent which can be determined from creep deformation map, the author found that the deformation mechanism is dislocation creep, so n is between 5 and 7. Q is the activation energy, R is the universal gas constant, and T is the temperature (K).

For predicting the fatigue life of solder joints, four fatigue life empirical equations are used to determine the fatigue lives of the solder joint alloys considered in this work. The output such as plastic strain, plastic shear strain, shear strain, accumulated creep density and creep energy density parameters are determined from ANSYS using the

Anand model in Eq. 2. Supplementary data on the fatigue lives of solder joint alloys are presented in the authors' publications [6]–[8], [10].

- Anand Model, $\dot{\varepsilon}^{p} = Aexp\left(-\frac{Q}{RT}\right)\left(sin\mathrm{h}\left[\xi\frac{\bar{\sigma}}{s}\right]\right)^{\frac{1}{m}}$ (2)

- Engelmaier equation, $\mathrm{N_f} = \frac{1}{2}\left(\frac{\Delta\gamma}{2\varepsilon_f'}\right)^{\frac{1}{c}}$ (3)
- Coffin-Manson equation, $\mathrm{N_f^m}\Delta\varepsilon_p = c$ (4)
- Solomon equation, $\Delta\gamma_p \mathrm{N_f^{\alpha}} = \theta$ (5)
- Syed equation, $\mathrm{N_f} = (\mathrm{W'}\omega_{acc})^{-1}$ (6)

2.2.2 Loading and Boundary Conditions

Two specific loading conditions used in this investigation are isothermal ageing and thermal cycling. The temperature loading started from 22℃, dwelled at -40℃, at the rate of 15℃ /min and ramped up to 22℃, for 1,380 s and excursion temperature (ET) of 150℃, for 1,908 s where it dwelled for 600 s. The solder joints are aged at -40℃, 25℃, 75℃ and 125℃ for 45 days (64,800 mins) in an ANSYS simulation environment. The FE models were subjected to six complete ATCs in 36 steps presented in the thermal cycling plot (Fig. 2). In addition, the models are subjected to standard IEC 60749-25 temperature cycling in ANSYS mechanical package environment. The solder joints are at homologous temperature during the loading. The assemblies were supported such that the conditions of the structure at the supports are:
At the PCB base, $y = 0$, and $u_{(y)} = 0$; Top surface $u_{(y)} = 0$, $u_{(x)}$ and $u_{(z)}$ are free.
The $u_{(x)}$, $u_{(y)}$ and $u_{(z)}$ represents the displacement in the x, y and z directions, respectively. Thus, the bottom surface of the PCB was fixed in Y direction and displaced in the X and Z directions.

2.2.3 Basic Assumptions

The basic assumptions employed in the FEA research methodology include:

- All the materials were modelled as linear elastic and isotropic materials except the solders and PCB, simulated using the Garofalo creep relations and orthographic materials.
- All materials, including the solder joint, were assumed homogeneous at load steps.
- The assemblies were assumed to be stress-free at room temperature, which was also the starting temperature of the thermal cycle loading.
- The material property of the solder bump is non-linear and temperature-dependent. In other words, others are linear and temperature-independent.
- Every interface of the materials is assumed to be in contact with each other.

2.2.4 Failure Criterion

The generally used solder-joint failure criteria include those based on plastic strain [11]–[13], creep strain [14]–[16], inelastic work [17], [18], classic fracture mechanics [19], and fracture-calibrated energy [20]. Each failure criterion requires specific material properties and could place the requirements on the type of the mathematical solution acquired either by calculation or in FEA simulation for the five solder joint alloy materials (lead-based eutectic Sn63Pb37, and lead-free SAC305, SAC387, SAC396 and SAC405) considered in this study.

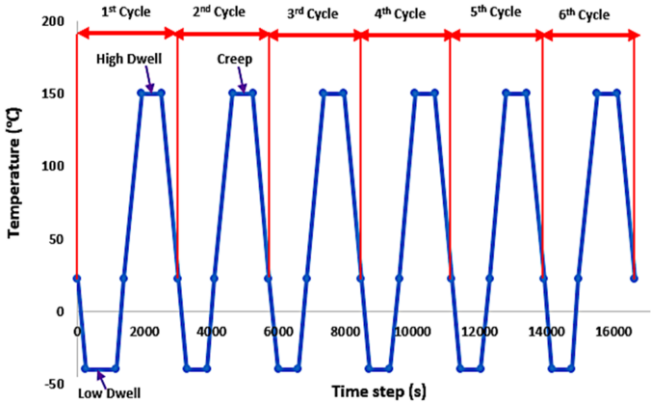

Figure 2: Thermal cycling plots used in the ANSYS FEA simulation

3.0 Results and Discussions

The results of this investigation are presented under two key headings. These are the effect of isothermal ageing and thermal cycling loading:

3.1 Effect of isothermal ageing on solder creep response

Isothermal loading increases creep damage in solder joints. Creep deformation tends to occur at an actual rate when the homologous temperature is ~0.5 or higher. The FEA simulation results show that creep occurs faster at higher temperatures. Similarly, it was understood that stress increases with the rate of deformation. Critical strain magnitude appears at the top and bottom of the solder joints at a high homologous temperature, decreasing gradually as the temperature decreases. The author investigated the effect of isothermal ageing on creep response in four different contexts. These are examined thus:

3.1.1 Effect of isothermal ageing on creep response on solder equivalent total strain

The outcomes obtained for the simulated FE model's equivalent strain are presented in Fig. 3, while Fig. 4 shows schematic strain distribution.

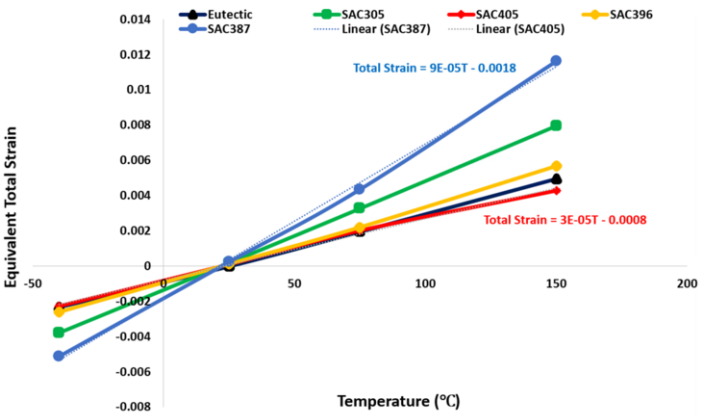

Figure 3: Plot of strain rate vs temperature for eutectic lead-based Sn63Pb37 and lead-free SAC solders subjected thermal ageing

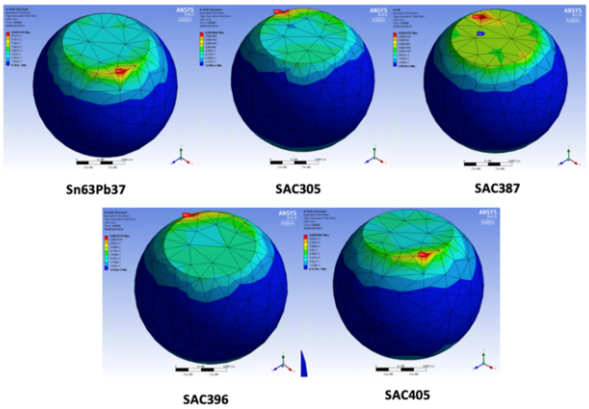

Figure 4: Schematic of equivalent total strain for lead-based eutectic Sn63Pb37 and lead-free SAC solders after isothermal ageing modelling

Table 1: Empirical Mathematical relationships for untried temperature, T

Solder Alloys	Empirical Equations
Sn63Pb37	$E_d = 9 \times 10^{-5}T^2 + 0.0064T - 0.4012$
SAC305	$\sigma = 3.152T - 68.167$
SAC387	$\varepsilon = 9 \times 10^{-5}T - 0.0018;\ E_d = 0.0003T^2 + 0.0483T - 1.2915$
SAC396	$E_d = 0.0001T^2 + 0.0073T - 0.4515;\ \varepsilon = 4 \times 10^{-5}T - 0.0009$ $\sigma = 1.8684T - 40.1$
SAC405	$\varepsilon = 3 \times 10^{-5}T - 0.0008;\ E_d = 0.0001T^2 + 0.0073T - 0.4515$ $\sigma = 1.543T - 34.983$

ε = Equivalent Strain, σ = Equivalent Stress, T = Untried Temperature and E_d = Strain Energy Density

The author observed from Fig. 3 that SAC405 accumulated the lowest strain rate, whereas SAC387 has the highest strain rate as the ageing temperature increases. As expected, as the temperature increases, the material decline's strength and modulus, imitating changes in the strain rate. One significant conclusion from the outcomes is that solder joints failure is highly strain rate dependent. Fig. 4 show the regions on the solder bump with a high strain rate that induces creep failure. This study has determined empirical equations valuable for engineers and academic communities. Table 1 shows sets of empirical equations useful for engineers, electronics manufacturing industries, and educational establishments to assess the stress, strain, and strain energy density of untried or unknown temperatures in electronics packages.

3.1.2 Effect of isothermal ageing on creep response on solder strain energy density

The strain energy dissipated in solder joints during thermal ageing has been investigated by FE simulation using ANSYS software for 45 days. It is seen that the lead-based eutectic Sn63Pb37 solder has the lowest strain energy density, followed by the SAC405 solder. On the other hand, SAC387 accumulated the highest strain energy and, consequently, more susceptive to failures than the rest of the solders studied. By using FEA, the time-dependent creep strain energy for the different solders is quantified. The results corroborate that induced strain energy density impacts the solder joints during operations. The higher the strain energy density, the more critical the joints' accumulated strain leads to creep fatigue failure. This implies that strain energy in the solder joints impacts the thermo-mechanical reliability of the BGA assembly joints.

3.1.3 Effect of isothermal ageing on creep response on solder total deformation

The total deformation obtained is the vector sum of all directional displacements of the solder assembly. The deformation outcomes for the solders studied in this investigation indicates that SAC387 has the highest deformation rate, while SAC405 accumulates the lowest deformation rate. The higher the free deformation, the less the stress accumulated in the solder joints.

3.1.4 Effect of isothermal ageing on creep response on solder Von Mises stress

The Von Mises stress in the solder joint is a measure of creep degradation of the joint. It is discovered that the magnitude of stress at 25℃ is low compared to other temperatures. The low value is attributed to the limited ability of solder to creep at low temperatures. The SAC405 is seen to have the lowest equivalent stress, followed by the SAC396 solder. On the other hand, the SAC305, eutectic Sn63Pb37 and SAC387 solders have the highest Von Mises stress. The stress evaluation founds that the crack is initiated at the top and bottom of the solder bumps, which depicts the stress distribution gradient.

3.2 Effect of thermal cycling on solder creep response

Like the discussion on isothermal loading, thermal cycling analysis on solder creep response is studied and presented in three frameworks. These are examined thus:

3.2.1 Effect of thermal cycling on creep response on solder Von-Mises stress

Cyclic thermal stresses in electronic packages have been identified as a fundamental challenge to electronic reliability. The reliability is associated with crack initiation and propagation, which culminates in systems failure if not controlled. The simulation output results are used to plot Figs. 5 and 6. Fig. 5 shows that SAC305 has the highest stress magnitude, while SAC405 has the lowest magnitude. Hence, the author could deduce that SAC405 is the most stable and less likely to attain its yield stress. Fig. 6 shows that the stress is critical at the edges of the solder bump, and thus, crack is most probable to nucleate there.

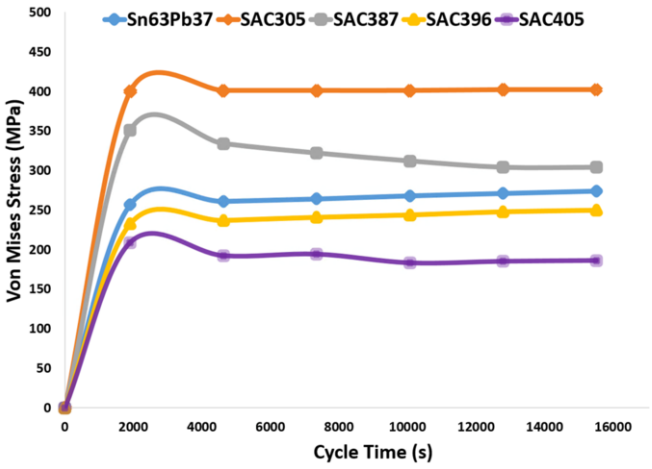

Figure 5: Plot of Von Mises stress for lead-based eutectic Sn63Pb37 and lead-free SAC solders subjected thermal cycling

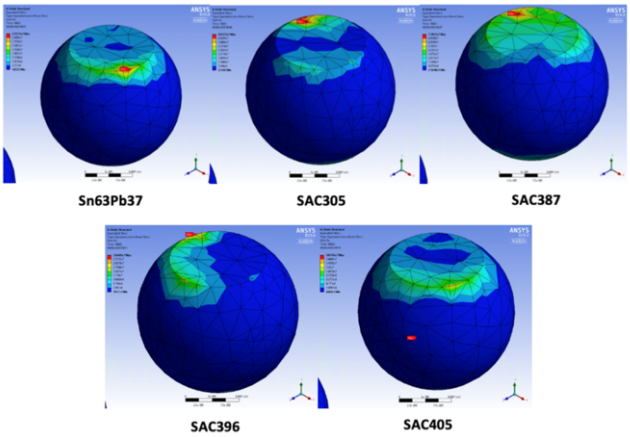

Figure 6: Schematic of Von Mises stress for lead-based eutectic Sn63Pb37 and lead-free SAC solders subjected to thermal cycling modelling

3.2.2 Effect of thermal cycling on creep response on solder strain rate

The simulation's strain rate outputs show that SAC387 and SAC405 are the highest and least strained solder alloys. The inference is that SAC405 is the most stable during the thermal cycle loading, while SAC387 is the least stable.

3.2.3 Effect of thermal cycling on creep response on solder strain energy density

The FEA simulation results obtained for the solders' strain energy density show that the creep strain energy's magnitude varies for different solder alloys used in the research. For example, the author observes that SAC387 has the highest strain energy density while lead-free SAC405 and lead-based eutectic Sn63Pb37 have the lowest strain energy.

3.3 Stress-Strain Hysteresis Loop Relationship and Thermal Fatigue Life Predictions for Solder Joint

Another way to assess the stress-strain relationship and capture continuous viscoplastic effects during thermal cycles is to plot the stress-strain hysteresis loop, as presented in Fig. 7. The figure shows the hysteresis loop for lead-based eutectic Sn63Pb37 and lead-free SAC305, SAC396, SAC387 and SAC405 solder alloys. The plot shows that the higher the stress magnitude, the larger the area of dissipated work at individual cycle, which indicates that the more significant the damage through each cycle, the smaller the cycle to failure. Therefore, the hysteresis loop area is an important parameter required to evaluate the fatigue life of solder joints. For example, from the hysteresis loop plot presented in Fig. 8, it could be seen that the stress-strain hysteresis loop shows that SAC405 has the lowest strain energy per unit volume absorbed, followed by SAC396, eutectic Sn63Pb37, and SAC305. On the other hand, SAC387 has the highest strain energy per unit volume. This premise shows that the hysteresis loop is a more valuable tool to gauge the degree of failure in the solder alloys, estimating crack growth rate and lifetime.

The prediction models are significantly not consistent in predicted magnitudes of TFLs across the solder joints. However, with circa 838% variation in the magnitudes of TFL predicted for Sn63Pb37, the damage parameters used in the models played a critical role and justifies that a combination of several failure modes drives solder joints damage.

The SAC405 joints have the highest predicted TFL of circa 13.2 years, while SAC387 joints have the least life of circa 1.4 years (Fig. 8). In addition, the SAC405 solder joints accumulated the lowest stress, plastic strain, and creep energy density magnitude, thus the highest fatigue life. The outcomes show that the SAC305 solder joint has a margin of error ±12% higher than those reported by the investigators why SAC387 is within the margin of error of 18.5% lower than the result obtained by Tao et al. [21] for the SAC387 solder alloys than those obtained in this work. This shows comparable relations between the researchers' results and the findings from this work.

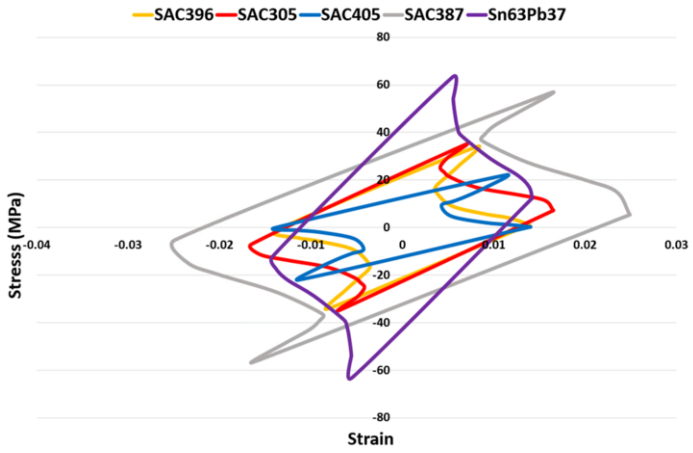

Figure 7: Stress-strain hysteresis loop for solder alloys

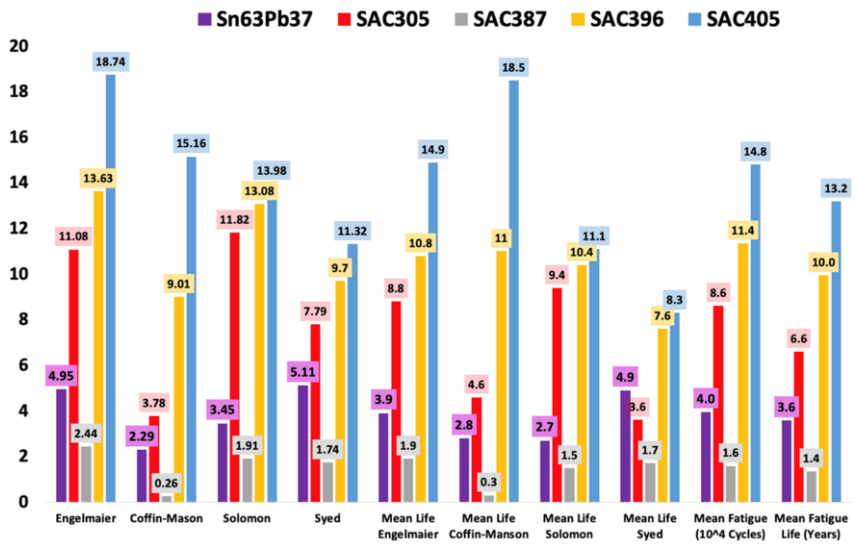

Figure 8: Fatigue lives of BGA solder joint alloys

4.0 Conclusions

The lead-free SAC405 was determined to possess the least stress magnitude, strain rate, deformation rate and strain energy density than the other solder joint alloys investigated in this work. The creep induced fatigue failure is more apparent in the SAC387 and Sn63Pb37 solder joint alloys, respectively. Additionally, the hysteresis loops show that the SAC405 solder has the lowest dissipated energy per cycle; thus, the highest fatigue life, followed by SAC396.

The SAC405 joints have the highest predicted TFL of circa 13.2 years, while SAC387 joints have the least life of circa 1.4 years. The predicted lives are inversely proportional to the magnitude of the areas of stress-strain hysteresis loops of the solder joints. The observation recognises a significant variation in the models' predicted values - justifying that several failure modes drive solder joints' damage mechanics.

This research is limited to lead-based eutectic Sn63Pb37 and four lead-free (SAC305, SAC387, SAC396 and SAC405) solder alloys. Also, for the creep-fatigue behaviour of solder joints, the author bases the failure criterion on stress, strain, strain energy density, deformation, and stress-strain hysteresis loop. The author also used these four fatigue life models because of their accuracy, effectiveness, and the most convenient tool used to calculate the thermal fatigue life of solder joints and predict useful life cycle and lifetime of solder joint compared to other fatigue life models. An experimental determination of the effect of thermal cycling and isothermal ageing with the five solder joint alloys considered in this work will have to be carried out at various temperatures applied in this research.

It is concluded that plastic strain, shear strain, plastic shear strain, accumulated creep energy density, and creep energy density for failures are damage parameters used to determine the solder's thermal fatigue lives of solder joint alloys in electronic assemblies. As a result, SAC405 and SAC396 are the best solder alloys in thermo-mechanical loading conditions when creep-fatigue behaviours are desired.

Acknowledgement

The work reported in this article is funded by the School of Mechanical Engineering & the Built Environment, College of Engineering & Technology, University of Derby, UK.

References

[1] K. Kanlayasiri and K. Sukpimai, "Effects of indium on the intermetallic layer between low-Ag SAC0307-xIn lead-free solders and Cu substrate," *J. Alloys Compd.*, 2016, doi: 10.1016/j.jallcom.2016.01.231.

[2] R. J. Coyle, K. Sweatman, and B. Arfaei, "Thermal Fatigue Evaluation of Pb-Free Solder Joints: Results, Lessons Learned, and Future Trends," *JOM*, vol. 67, no. 10, pp. 2394–2415, 2015, doi: 10.1007/s11837-015-1595-1.

[3] J. Zhang, Z. Hai, J. L. Evans, M. J, J. C, and A. Silver, "Correlation of Aging Effects on Creep Rate and Reliability in Lead Free Solder Joints," *SMTA J.*, vol. 25, no. 3, pp. 19–28, 2012, [Online]. Available: http://www.smta.org/knowledge/journal_detail.cfm?ARTICLE_ID=205&RENEWAL_DATE=03/01/2016&MEM_TYPE_ID=8&CFID=99964&CFTOKEN=13964490&jsessionid=8792441708208D293AA47045E7E7AE35.cfusion.

[4] C. Basaran, H. Ye, D. C. Hopkins, D. Frear, and J. K. Lin, "Failure modes of flip chip solder joints under high electric current density," *J. Electron. Packag. Trans. ASME*, 2005, doi: 10.1115/1.1898338.

[5] J. Gomez and C. Basaran, "Damage mechanics constitutive model for Pb/Sn solder joints incorporating non-linear kinematic hardening and rate dependent effects using a return mapping integration algorithm," *Mech. Mater.*, vol. 38, no. 7, pp. 585–598, 2006, doi: 10.1016/j.mechmat.2005.11.008.

[6] J. A. Depiver, S. Mallik, and E. H. Amalu, "Creep Response of Various Solders used in Soldering Ball Grid Array (BGA) on Printed," *IAENG*, vol. 0958, 2019.

[7] J. A. Depiver, S. Mallik, and E. H. Amalu, "Effective Solder for Improved Thermo-Mechanical Reliability of Solder Joints in a Ball Grid Array (BGA) Soldered on Printed Circuit Board (PCB)," *J. Electron. Mater.*, 2020, doi: 10.1007/s11664-020-08525-9.

[8] J. Adeniyi Depiver, S. Mallik, and E. H. Amalu, "Comparing and benchmarking fatigue behaviours of various SAC solders under thermo-mechanical loading," 2020, doi: 10.1109/ESTC48849.2020.9229699.

[9] F. Garofalo and D. B. Butrymowicz, "Fundamentals of Creep and Creep-Rupture in Metals," *Phys. Today*, 1966, doi: 10.1063/1.3048224.

[10] J. A. Depiver, S. Mallik, and E. H. Amalu, "Thermal fatigue life of ball grid array (BGA) solder joints made from different alloy compositions," no. April, pp. 1–26, 2021.

[11] L. F. Coffin, "A study of the effects of cyclic thermal stresses on a ductile metal," *Transactions of the American Society of Mechanical Engineers*. 1954.

[12] S. Wiese and S. Rzepka, "Time-independent elastic-plastic behaviour of solder materials," 2004, doi: 10.1016/j.microrel.2004.04.015.

[13] D. R. Shirley, H. R. Ghorbani, and J. K. Spelt, "Effect of primary creep and plasticity in the modeling of thermal fatigue of SnPb and SnAgCu solder joints," *Microelectron. Reliab.*, 2008, doi: 10.1016/j.microrel.2007.08.002.

[14] B. Wong, D. E. Helling, and R. W. Clark, "A Creep-Rupture Model for Two-Phase Eutectic Solders," *IEEE Trans. Components, Hybrids, Manuf. Technol.*, 1988, doi: 10.1109/33.16655.

[15] A. Syed, "Accumulated creep strain and energy density based thermal fatigue life prediction models for SnAgCu solder joints," 2004, doi: 10.1109/ectc.2004.1319419.

[16] M. M. Hasnine, J. C. Suhling, B. C. Prorok, and M. J. Bozack, "the Mechanical Behavior of Ceramic," *2007 Proc. 57th Electron. Components Technol. Conf.*, vol. 37, no. 7, pp. 49–53, 2014, doi: 10.1109/ECTC.2014.6897315.

[17] J. Morrow, "Cyclic Plastic Strain Energy and Fatigue of Metals," in *Internal Friction, Damping, and Cyclic Plasticity*, 2009.

[18] F. Ellyin and D. Kujawski, "Plastic strain energy in fatigue failure," *J. Press. Vessel Technol. Trans. ASME*, 1984, doi: 10.1115/1.3264362.

[19] J. H. Lau and Y. Pao, *Solder joint reliability of BGA, CSP, Flip Cip, and fine pitch SMT assemblies*. 1997.

[20] R. Darveaux, K. Banerji, A. Mawer, G. Dody, and J. Lau, "Reliability of plastic ball grid array assembly. In Ball grid array technology (Vol. 13, pp. 379-442). McGraw-Hill.," *Ball grid array Technol. McGraw-Hill*, vol. 13, pp. 379–442, 1995.

[21] Q. B. Tao, L. Benabou, V. N. Le, N. N. Anh, and T. N. Hung, "Temperature-dependent fatigue modelling of a novel Ni, Bi and Sb containing Sn-3.8Ag-0.7Cu lead-free solder alloy," *Fatigue Fract. Eng. Mater. Struct.*, vol. 43, no. 12, pp. 2883–2891, 2020, doi: https://doi.org/10.1111/ffe.13313.